SURFACE-RELATED PROPERTIES AS AN ESSENTIAL INGREDIENT TO ELECTRON-CLOUD SIMULATIONS

Roberto Cimino*, LNF-INFN I-00044 Frascati, Italy

Abstract

In recent years e-cloud related processes have been understood to play a major role in limiting the expected performances of some present and planned accelerators. Big efforts have been than devoted to the detailed comprehension of the process and more and more refined simulation codes have been produced in order to be able to predict and control such effects. Essential input parameters to such calculations are a number of surface related properties which detailed study has attracted growing attention.

In this context surface science studies can address a number of important issue like photo and electron reflectivity, photo and electron induced electron emitted energy spectrum, surface changes as induced by photon or electron bombardment etc. Here we present some experimental results of interest to e-cloud studies performed by means of state of the art surface science techniques.

INTRODUCTION

The build-up of an electron cloud and beam induced electron multipacting was first observed in the ISR more than 25 years ago [1]. Since then, a significant theoretical effort has been made to understand and predict electron cloud phenomena and its impact on various machines [2]. In addition, a number of experimental observations of electron cloud effects have been reported to occur on different accelerators [2]. In this paper we consider the Large Hadron Collider to be built at CERN (Geneva) as a test case to describe surface properties of importance to determine e-cloud effects in the machines. Similar results should be carefully obtained for each planned accelerators in order to correctly simulate e-cloud effects on beam instability in each case and for each material solution.

The LHC will provide two counter-circulating proton beams with colliding energies of nominally 14 TeV in the centre of mass, requiring superconducting bending magnets operating in super-fluid helium at 1.9 K. In order to reduce the cryogenic power consumption at 1.9 K in the arcs, the heat load induced by the beam will be intercepted on a beam screen, which operates between 5 and 20 K. In the arcs of the machine, desorbed molecules will be pumped through the pumping slots, distributed along the length of the beam screen, onto the surrounding cold bore held at 1.9 K.

Relevant to the building and the commissioning of the LHC, an on-going experimental and theoretical campaign was launched in 1997 to identify the potentially detrimental effects of electron cloud phenomena on the machine performance and to identify possible remedies [2].

A significant number of combined experiments and simulations observe and predict multipacting effects induced by the build-up of an electron cloud in the SPS once an LHC type beam is injected [3]. Such experiments and simulations also provide convincing evidence that the observed electron cloud effects are indeed to be expected in the LHC, not only inducing undesirable pressure rises, but more importantly affecting the acceptable heat load in the cryogenically cooled arcs of the machine [2].

Photo–reflectivity and emission and electron-induced secondary electron production are to be considered essential ingredients to be used in the simulation codes. We will describe in the following some state of the art experiment to quantitatively estimate the aforementioned surface parameters in the case of LHC.

PHOTON REFLECTIVITY

In the LHC, the emitted synchrotron radiation (SR) from the circulating protons, with a critical energy of 44.1 eV, is a major consideration for the design of the vacuum system. Its radiated power, induces a heat load of 0.2 W/m at 7 TeV per beam and may i) stimulate gas desorption of weakly and tightly bound gases from the walls of the vacuum system either directly by photons or mediated by electrons [4,5], ii) create photoelectrons [6] which can be accelerated, to an average energy of 90 eV, towards the opposite wall by the positive space charge of the bunched beam leading to additional gas desorption and heat loads on the cryogenic system, iii) create secondary electrons which may contribute to electron multipacting.

In the arcs, synchrotron radiation with a beam divergence of 0.55 mrad for 5 eV photons will illuminate the beam screen at a mean incidence angle of 4.5 mrad in the presence of a magnetic field of 8 T perpendicular to the orbit. Hence the electrons photo-emitted on the orbital plane, will be affected by the magnetic field, and constrained to move along the field lines, thus they will not be able to cross the vacuum chamber and gain energy from the beam. On the other hand, an electron emitted perpendicular to the orbital plane (hence parallel to the magnetic field) will only spiral along the field lines, participating more efficiently to secondary electron production and, eventually, to multipacting. This simple reasoning implies that it will be extremely beneficial to adsorb most of the SR on the orbit plane, where the created electrons cannot participate in the multipacting, rather than having them reflected on the top and bottom parts of the beam pipe. To this end, the LHC beam pipe has been designed and produced with a “saw-tooth”

* Roberto.Cimino@lnf.infn.it

structure on the equator where the photons first impinge, so as to offer to such a grazing incident SR a close to normal incidence impact, hence reducing its reflectivity. This study address quantitatively the photon reflectivity from the final production of co-laminated copper on stainless steel for the LHC beam screen (BS), including all cleaning stages, and surface preparation (both for the flat and the saw-tooth surface).

The reflectivity measurements were performed at the BEAR beamline at ELETTRA in Trieste. This is a bending magnet beamline, which can provide a monochromatic beam with energies from 8 to 1400 eV with a resolving power between 2200 and 5800 [7], and a white light with a spectral distribution similar to that of the LHC.

The experimental station has been described elsewhere [8]. The set-up allows to determine the space distribution of the scattered light by computer controlled movements of a calibrated photodiode (AXUV100 by IRD), over the entire space above the sample with the exception of the small region where the diode would have intercepted the incoming light. The complete solid angle above the sample has been divided in three different regions: the forward scattering region, 8°x8° around the centre of the geometrical reflection, the backscattered region, 36°x36° around the incoming light direction; the diffused region which sums up all the emitted photons outside the two aforementioned regions. Such separation, although useful to analyse the data and their impact to the study of LHC - BIEM related simulations, is somehow artificial and is made considering experimental constraints such as the photodiode physical dimensions and the expected spread and beam divergence.

In figure 1, the photon reflectivity of "white light" similar to the one emitted by LHC is shown as a function of the azimuthal position of the photodiode on the scattering plane. The blue box shows the reflectivity of the as-received flat Cu sample, while the red box shows the data collected on the saw-tooth Cu sample. Each box represents a single measurement of the drain photocurrent measured by the diode (which covers 8° in the azimuth angle of the scattering plane) and normalised to the incident light. In case of the flat Cu surface, most (80%) of the reflected light is collected by the photodiode when placed around the geometrically defined specular (i.e. forward) direction and only a very small part of the incident light is back reflected or diffused (less than 2 %). Probably part of the diffused component, being measured close to forward reflection, is produced by the intrinsic divergence of the reflected beam due to the roughness of the sample surface. The sum of all the measured reflectivity, with the photodiode spanning over the whole solid angle above the irradiated flat Cu sample, allow us to extract the total reflectivity of 82 % *i.e.* 18 % of the incoming light is absorbed. On the other hand, the forward scattering measured from the saw-tooth sample is only about 4 % while the total reflectivity, over the entire space, is around 10 % *i.e.* 90 % of the incoming light was absorbed. The residual forward scattering reflectivity of the saw-tooth structure may be explained by the presence of flat surface in the "crest" of the saw-tooth, which essentially act as the flat sample, but with a reduced active surface. The diffused and back-scattered components, on the other hand, are due to persistent reflectivity even close to normal incidence, as expected theoretically. Also in this case the diffused component measured closer to the geometrical specular reflection is probably due to a significant increase in beam divergence of the reflected beam caused by roughness and imperfection of the saw-tooth structure surface.

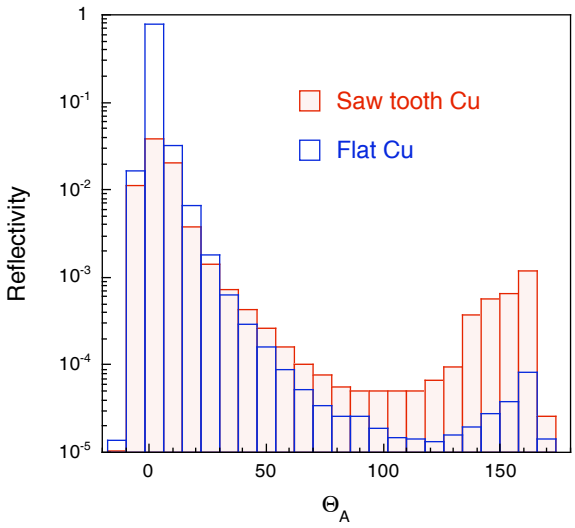

Figure 1: Measured reflectivity, on the scattering plane, from a flat Cu sample (blue empty bars) and from the saw-tooth sample (red bars).

The reduction of the total number of reflected photons by using the saw-tooth structure is significant, and only apparently increases the light diffused or backscattered. Given the horizontal and vertical divergence of the beam impinging on the wall, if no saw-tooth structure were foreseen, the vacuum chamber would be evenly illuminated by the forward reflected light after a few reflections, giving a diffused photon background between 40 to 60 %, that is much higher than that resulting from back and diffused scattering from the saw-tooth structure.

It is also possible to determine the spectral distribution of the reflected/diffused light by using monochromatic photons [8]. It is demonstrated that, in the case of the saw-tooth sample, the back-reflected and diffused light consist almost entirely of low-energy photons, while the forward-scattered light has an energy distribution very similar to that of the flat sample, indicating, as expected, that this sample behaves in forward direction as a very low efficiency flat mirror surface.

Considering the beam divergence in the closed system of the LHC, the saw-tooth structure reduces the number of photons impinging on the wall synchronously to the

proton beam (the forward reflected photons) by more than a factor 20, and significantly reduces the diffused light, which in the saw-tooth case mainly derive from backscattered photons, while in the flat surface case, would derive from multiple reflections of the naturally divergent forward-scattered beam. Our data confirm the validity of the adopted solution for LHC arcs beam screen and produce quantitative estimates of photon reflectivity to be used in BIEM calculation.

SECONDARY ELECTRON EMISSION

Simulations show [2] that electron cloud activity expected in the LHC does indeed induce an additional heat load depending on a number of the vacuum chamber material surface conditions and electronic properties. To correctly predict such extra heat load, it is then essential to determine accurately the secondary electron yield (SEY) at cryogenic temperatures (eventually in presence adsorbed gas), the energy distribution of the emitted electrons as excited by photons and by electrons and the ratio between true secondaries and reflected electrons.

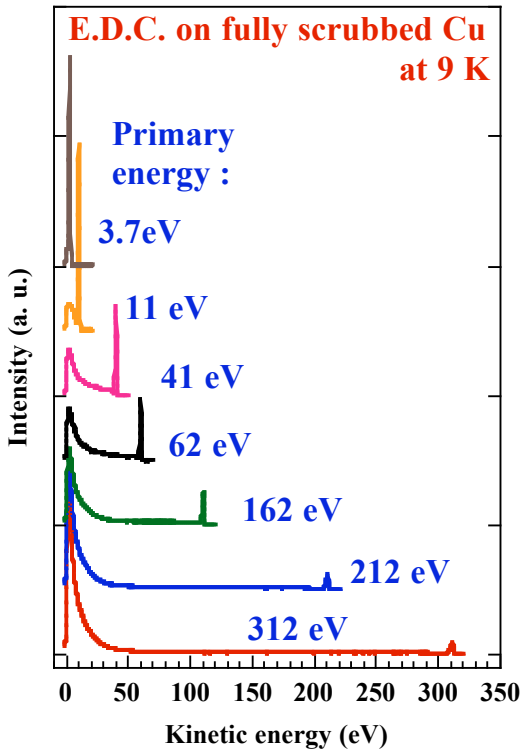

Figure 2: Some selected EDC of fully scrubbed Cu surface at ~10 K as a function of impinging primary electron energy.

Here we focus mainly on electron induced electron Energy Distribution Curves (EDC) from low temperature surfaces (~10K) and try to disentangle in those EDC the percentage of reflected electrons contributing to the total SEY. Particular attention was paid to the effects of low energy electrons (from 0 to around 50 eV) since it has been reported that the energy distribution of the electrons impinging on the wall and playing a role in inducing electron cloud effects is peaked at very low energy (from 0 to 20 eV) and does not extend significantly over 300 eV [2].

The analyses of the electron induced electron EDC at low primary energy requires a suitable experimental set-up which has been described elsewhere [9]. It allows to collect angle integrated EDC with a low energy (30 to 350 eV), small (less than a 1 mm^2) and stable (both in current and position) focused beam. The sample studied are representative for the real surface 'seen' by the proton beam in the machine and its temperature can range between 8 and 400 K. To measure low energy (close to 0 eV) impinging primary electrons, a bias voltage was applied on the sample.

In fig.2 we report a sub-set of EDC taken as a function of primary energy from an as-received Cu, held at ~10 K. Since it has been shown that electron bombardment can modify a surface and its SEY, [2,10] we collected all our data from a stable surface (fully scrubbed) obtained by dosing with more than $1x10^{-2}$ C/mm^2 400 eV electrons. From the available data it is possible by simple numerical integration, to extract the ratio between secondary and reflected electrons for each primary energy. We consider all the electrons emitted between 0 eV and the onset of the clear peak at the energy of the primary electron beam are secondary electrons, while the integral under the peak gives the amount of electrons specularly reflected.

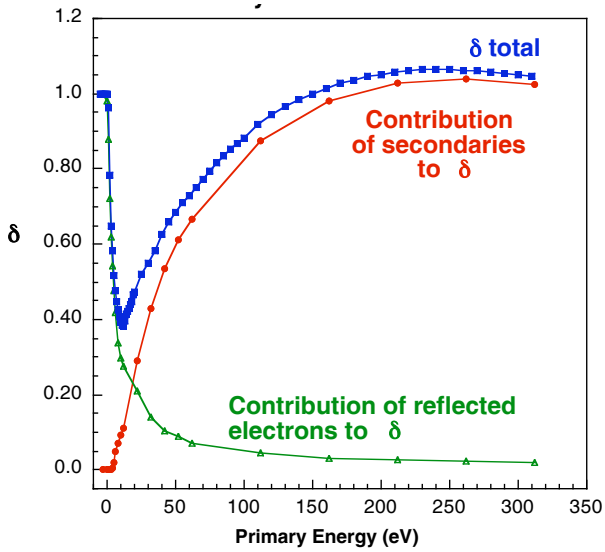

Figure 3: Total SEY (δ) and contribution to it of secondaries and reflected electrons from a fully scrubbed Cu surface at 9 K as a function of primary electron energy.

Performing this analysis at all measured energies it is then possible to extract the percentage of reflected and secondary electron component in the EDCs as a function of primary energy. This is shown in fig. 3 superimposing it to the actual SEY measured with a more direct technique on the same sample and in identical conditions

used to measure the EDC [9,11]. From the SEY data and the superimposed contributions of the reflected electron and the secondary electron components, we can clearly conclude that, at low energy most of the impinging electrons are reflected by the Cu surface, giving a SEY close to unity approaching primary electron beam zero energy. Our data suggest, for the first time in this context, that very low electrons may have long survival time inside the accelerator vacuum chamber due to their high reflectivity. This notion may well explain why in the KEK B factory [12] and SPS [3] a memory effect has been observed. Namely, the electron cloud build-up during the passage of a batch is enhanced by the passage of the preceding batches even if the time interval between the two trains is quite long (as long as 550 ns in the SPS). Implementing these experimental data into BIEM simulations indicate an increased heat load for the LHC [11].

CONCLUSION

In conclusion, these data suggest the need to use state of the art surface science set-up and techniques to measure input parameters to EC simulations and to address the different issues involving the intimate properties of accelerators surface walls, which are now being considered as essential parameters for determining the ultimate performances of present and future accelerators.

ACKNOWLEDGMENTS

The author acknowledge the basic contribution of I.R. Collins to most of the presented material, thanks CERN for hospitality and is indebted to V. Baglin, N. Hilleret, and P. Strubin for fruitful discussions.

REFERENCES

[1] O. Gröbner 10th international conference on High Energy Accelerators, Protvino, July 1977.
[2] See Proc. ECLOUD'02, CERN, Geneva, April 15-18, CERN-2002-001 (2002).
[3] J.M. Jiménez et al., CERN-LHC project report 632 (2003).
[4] J.Gómez-Goñi, O. Gröbner and A. G. Mathewson, J. Vac. Sci. Technol. **A12**(4), 1714 (1994).
[5] O. Gröbner, Vacuum **47**, 6-8, 591 (1996), and Proc. PAC97, Vancouver, 1997.
[6] R. Cimino, V. Baglin and I. R. Collins, PRST-AB **2**, 063201 (1999).
[7] http://bear.tasc.infm.it
[8] N. Mahne, V. Baglin, I. R. Collins. A. Giglia, L. Pasquali, M. Pedio, S. Nannarone, R. Cimino, Appl. Surf. Sci. **235**, 221 (2004).
[9] R. Cimino and I. R. Collins, Appl. Surf. Sci. **235**, 231 (2004).
[10] B. Henrist, N. Hilleret, C. Scheuerlein, M. Taborelli, G. Vorlaufer, LHC P.R. 583, and Proc. EPAC 2002.
[11] R. Cimino, I. R. Collins, M. A. Furman, M. Pivi, F. Ruggiero, G. Rumolo and F. Zimmermann, PRL **93** 14801 (2004)
[12] T. Miyajima et al. PAC 2003.